Stochastic Analysis of a Three-Phase Fluidized Bed: Fractal Approach

Three-phase fluidized beds have played important roles in various areas of chemical and biochemical processing. The characteristics of such beds are highly stochastic due to the influence of a variety of phenomena, including the jetting and bubbling of the fluidizing medium and the motion of the fluidized particles. A novel approach, based on the concept of fractals, has been adopted to analyze these complicated and stochastic characteristics. Specifically, pressure fluctuations in a gas-liquid-solid fluidized bed under different batch operating conditions have been analyzed in terms of Hurst's rescaled range (R/S) analysis, thus yielding the estimates for the so-called Hurst exponent, H. The time series of the pressure fluctuations has a local fractal dimension of $d_{FL} = 2 - H$. An H value of $1/2$ signifies that the time series follows Brownian motion; otherwise, it follows fractional Brownian motion (FBM), which has been found to be the case for the three-phase fluidized bed investigated.

L. T. Fan
Department of Chemical Engineering

D. Neogi
M. Yashima
R. Nassar
Department of Statistics
Kansas State University
Manhattan, KS 66506

Introduction

Gas-liquid-solid fluidized beds have emerged in recent years as one of the most promising devices for three-phase operations. Such devices, illustrated in Figure 1, are of considerable industrial importance as evidenced by their wide use for chemical, petrochemical and biochemical processing (see, e.g., Fan and Newcomer, 1981). As three-phase reactors, they have been employed in hydrogenation and hydrodesulfurization of residual oil for coal liquefaction, in turbulent contacting absorption for flue gas desulfurization, and in the bio-oxidation process for waste water treatment (see, e.g., Shah, 1981). Three-phase fluidized beds are also often used in physical operations. Publications on gas-liquid-solid fluidized beds have been reviewed extensively (see, e.g., Ostergaard, 1971; Epstein, 1981, 1983; Muroyama and Fan, 1985), the majority of which are concerned mainly with the deterministic or global properties of such beds. Thus, it is of paramount importance that we understand static and dynamic characteristics of the three-phase fluidized beds if they are to be adopted as chemical reactors. Such static and dynamic characteristics manifest themselves as the fluctuations of their properties, including density and pressure.

Fluidized beds or fluidized-bed reactors behave highly randomly or stochastically due to the influence of a variety of phenomena, including the jetting and bubbling of the fluidizing medium and the motion of the fluidized particles; pressure fluctuations are direct consequences of these phenomena. It was, therefore, natural that statistical methods were employed extensively to investigate the pressure fluctuations in fluidized beds. The earliest attempts were to define indices for the quality of fluidization through statistical analysis of the pressure fluctuations (Shuster and Kisliak, 1952; Bailie *et al.*, 1961; Sutherland, 1964; Winter, 1968; Moritomi *et al.*, 1980). Whitehead *et al.* (1977) have indicated that analyzing the pressure fluctuations in a fluidized bed yields information useful for devising control strategies for the bed. Swinehart (1966) has calculated the cross-correlation function between two pressure fluctuating signals taken from two vertically separated pressure taps and determined the "correlation-average propagation velocity" of bubbles in a fluidized bed. Kang *et al.* (1967), Lirag and Littman (1971), and Fan *et al.* (1981) have calculated the probability density, autocorrelation and power spectral density functions of the pressure fluctuations off-line. The resultant autocorrelation and power spectral density functions were then used to determine the frequency of the fluctuations. Among the stochastic models, one of the most notable has been the model proposed by Yutani *et al.* (1983). Both Yutani *et al.* (1983) and more recently Neogi *et al.* (1988) have considered that any of the pressure fluctuation signals from fluidized beds consists of two components, a periodic component, and a random component; the latter is modeled as a continuous-time Markov process.

Correspondence concerning this paper should be addressed to L. T. Fan.

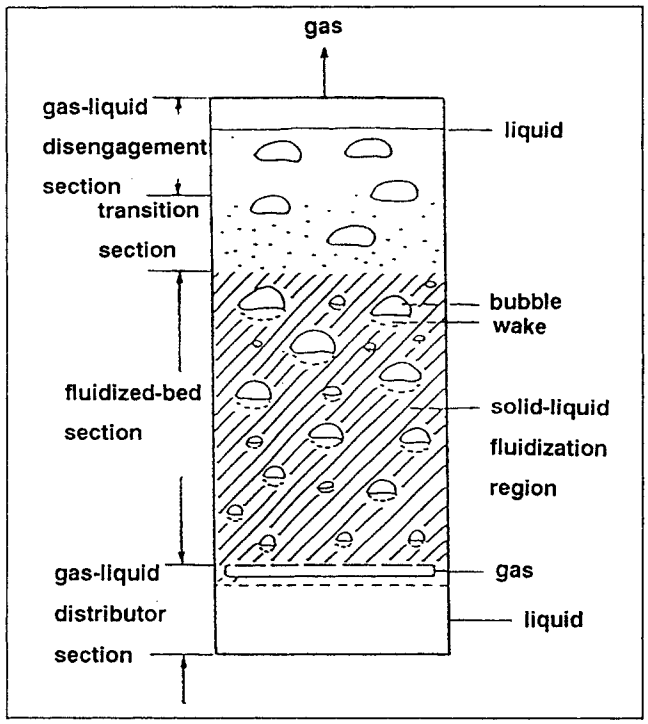

Figure 1. Three-phase fluidized-bed reactor.

While all these investigators demonstrated the power of the statistical method and stochastic modeling in successfully analyzing the random pressure fluctuations in a fluidized bed, the majority of them apparently dealt only with two-phase fluidized beds. Relatively little has been done to stochastically model the phenomena of pressure fluctuations in fluidized beds or three-phase fluidized-bed reactors.

While analyzing various hydrological data, Hurst (1956) has realized that numerous records of observations over time exhibit anomalous characteristics of what came to be known as the "Hurst Phenomenon." Our exhaustive review of the available data and the results of our experiments have indicated that the time series of pressure fluctuation signals from a fluidized bed exhibits long-term correlation similar to that observed in many hydrological time series. So far the Markov processes, including the Brownian motion, have played dominant roles in modeling the pressure fluctuations in fluidized beds (see, e.g., Yutani *et al.*, 1983; Neogi *et al.*, 1988). Nevertheless, they tend to underestimate long-term trends such as the range of "cumulative departure" from the mean as suggested by Hurst (1956). This observation is not surprising; a Markov process has a short-term memory with exponential decay, and Brownian motion comprises independent Gaussian white noise. In contrast, the fractional Brownian motion (FBM) model, proposed by Mandelbrot and van Ness (1968), is capable of identifying and interpreting long-term persistence or correlation in a time series. It is an extension of the central concept of Brownian motion that has played a significant role in both physics and mathematics; FBM has been one of the major contributions in the field of temporal fractals. This has led us to believe that deeper insights into the stochastic behavior of a three-phase fluidized bed can be gained by resorting to the concept of fractional Brownian motion.

In this paper, pressure fluctuations at various axial positions of a three-phase fluidized bed were measured by means of pressure probes over a range of time under various batch operating conditions. The resultant time series have been analyzed in terms of FBM, or more specifically, in terms of Hurst's rescaled range (R/S) analysis. This has yielded the estimates for the so-called Hurst exponent, H, and eventually the fractal dimension of the time series, d_{FL}.

Theoretical

The fractional Brownian motion model, proposed by Mandelbrot and van Ness (1968), is an extension of the central concept of Brownian motion; it is one of the major contributions in the field of temporal fractals. As can be seen from the sample traces presented in Figure 2 (Peitgen and Saupe, 1988), the fractional Brownian motion, $B_H(t)$, is a single-valued function of one variable, t (usually time). Formally, it is a sequence of the increments of FBM (i.e., $[B_H(t_2) - B_H(t_1)]$) that gives rise to noises, the sum of which produces each of the traces in Figure 2. The scaling behavior of the traces in this figure is characterized by the parameter, H, in the range, $0 < H < 1$. The traces with H close to 0 are most rugged while those with H close to 1 are relatively smooth. H relates the incremental change in $B_H(t)$, i.e., $\Delta B_H = B_H(t_2) - B_H(t_1)$, to the time difference, $\Delta t = t_2 - t_1$, through the simple scaling law, $\Delta B_H \propto (\Delta t)^H$. The increment, $[B(t + s) - B(t)]$, of the classical Brownian motion yields a Gaussian distribution with a variance proportional to the time lag, s; while the increment, $[B_H(t + s) - B_H(t)]$, of an FBM also yields a Gaussian distribution, its variance is proportional to s^{2H}. For $H = 1/2$, this obviously reduces to the result for the classical Brownian motion.

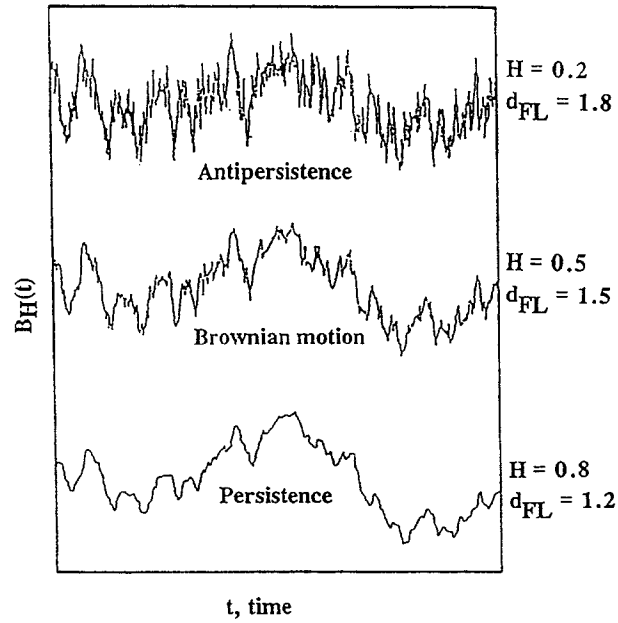

Figure 2. Sample plots of the fractional Brownian motion traces, $B_H(t)$, against t for different values of H and d_{FL}.

$\Delta B_H \propto t^H$.

From Peitgen and Saupe (1988)

The fractional Brownian motion, $B_H(t)$, is said to have a long run correlation; for $H > 1/2$, the increments of $B_H(t)$ are positively correlated (persistence), and for $H < 1/2$, the increments are negatively correlated (antipersistence). Note that for the singular case of $H = 1/2$, the correlation vanishes and gives rise to the well-known independent increment process of the classical Brownian motion.

Discrete-time fractional noise

A sequence of increments of $B_H(t)$, i.e., a sequence of values of $\Delta B_H(t) = B_H(t+1) - B_H(t)$ with integer values of time t, is termed "discrete-time fractional noise." For $H = 1/2$, $\Delta B_H(t)$ reduces to a discrete-time Gaussian white noise. Thus, for a record of time starting at time $t = 0$, we have $X(u) = B_H(u) - B_H(u-1)$ where $u = 1, 2, \ldots, s$ and $X(0) = 0$. Summing over u, we obtain

$$\sum_{u=1}^{s} X(u) = B_H(s) - B_H(0) = X^*(s) \qquad (1)$$

where s is the time lag. Thus, $X^*(s)$ is an increment of FBM, and $X(u)$ is a sequence of discrete-time fractional noises. If the recording of a signal is initiated at time t, then the definition of $X^*(s)$, Eq. 1, leads to

$$X^*(t+s) - X^*(t) = \sum_{u=1}^{t+s} X(u) - \sum_{u=1}^{t} X(u) = \sum_{u=1}^{s} X(t+u) \qquad (2)$$

The variance of this quantity is proportional to s^{2H}.

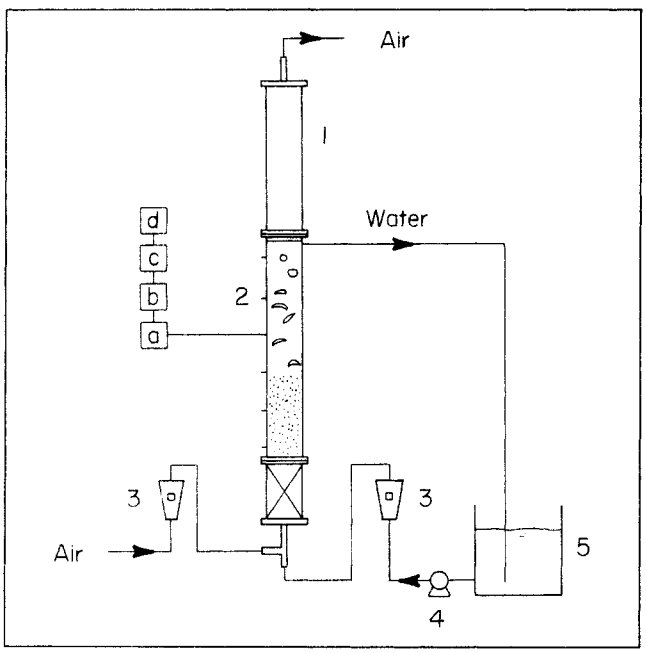

Figure 3. Experimental setup.

1. Main Column
2. Pressure Taps
3. Rotameter
4. Pump
5. Water Reservoir

a. Pressure Transducer
b. Amplifier
c. A/D Converter
d. Microcomputer.

Table 1. Properties of the Fluidizing Media and Fluidized Particles and Operating Conditions

Liquid Velocity (Water), m/s	0	0.056	0.076
Liquid Density (Water), kg/m^3		1.0×10^{-3}	
Gas Velocity (Air), m/s	0.0129	0.0366	0.0594
Gas Density (Air), kg/m^3		0.0012×10^{-3}	
Particle Diameter (Sand), m	0.00084	$-$ 0.00141	
Particle Density (Sand), kg/m^3		2.65×10^{-3}	
Static Bed Height, m		0.1016	
Probe Height, m	0.0413	0.1302	0.308

Rescaled range analysis

To obtain information about H for a given time series, we can resort to the rescaled range (R/S) analysis, which was originally proposed by Hurst (1956). Nevertheless, Mandelbrot and Wallis (1969a) were the first to apply this method to the determination of the fractal characteristics of a time series.

Let $X(u)$ be a record containing s readings uniformly spaced from time $u = t + 1$ to time $u = t + s$; $X(u)$ is a sequence of discrete-time fractional noises. Then, from Eq. 2,

$$\frac{1}{s}[X^*(t+s) - X^*(t)] = \frac{1}{s}\sum_{u=1}^{s} X(t+u) \equiv \langle X(t)\rangle_s \qquad (3)$$

which is the average of readings within the subrecord from time $t + 1$ to time $t + s$. Moreover, let $c(t, u)$ be the cumulative

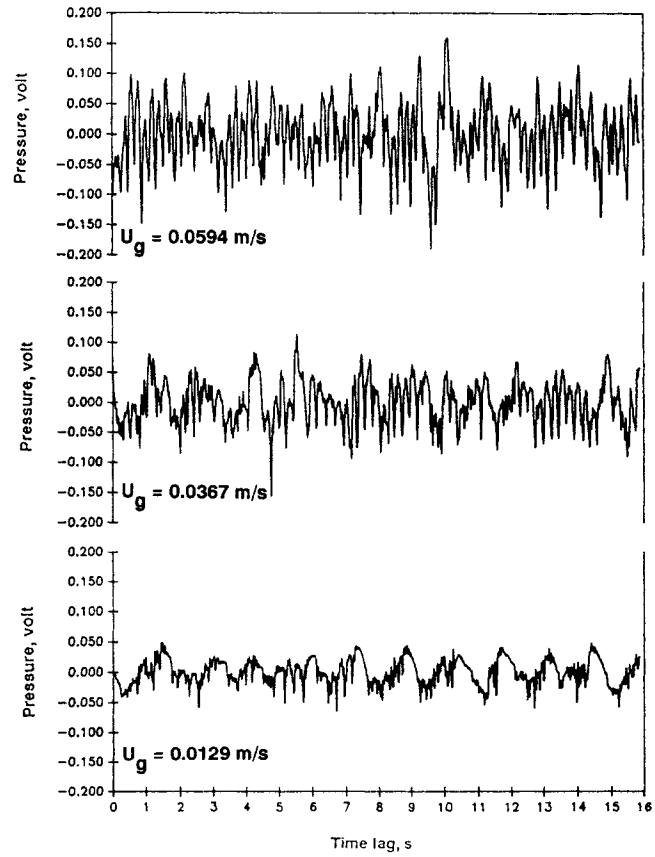

Figure 4. Typical pressure fluctuation signals at various superficial gas velocities.

U_l = 0.056 m/s; probe no. 2 (0.1302 m)

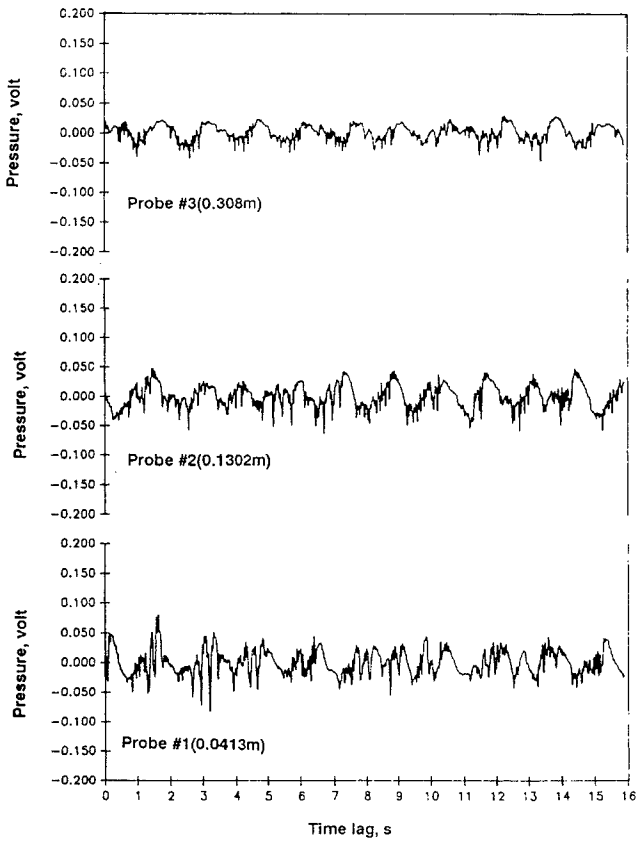

Figure 5. Typical pressure fluctuation signals at different probe heights.
$U_\ell = 0.056$ m/s; $U_g = 0.0129$ m/s

departure of $X(t + y)$ from the mean, $\langle X(t)\rangle_s$, for the sub-record, between time $t + 1$ corresponding to $y = 1$ and time $t + u$ corresponding to $y = u$; note that by definition,

$$c(t, u) = \sum_{y=1}^{u} [X(t + y) - \langle X(t)\rangle_s] \tag{4}$$

The sample sequential range of $X(t)$ for lag s is defined as

$$R(t, s) = \max_{0<u\le s} c(t, u) - \min_{0<u\le s} c(t, u) \tag{5}$$

and the sample sequential variance of $X(t)$, S^2, is defined as

$$S^2(t, s) = \frac{1}{s}\sum_{u=1}^{s} \{X(t + u) - \langle X(t)\rangle_s\}^2 \tag{6}$$

The ratio, $R(t, s)/S(t, s)$, is termed the rescaled range (Mandelbrot and Wallis, 1969a; Feder, 1988).

Hurst (1956) and later Mandelbrot and Wallis (1969a) have determined that $R(t, s)/S(t, s)$ is a random function with the scaling relationship (Mandelbrot and van Ness, 1968)

$$\frac{R(t, s)}{S(t, s)} \propto s^H \tag{7}$$

This scaling relationship is sometimes referred to as the "Hurst Law." Long-term persistence or correlation, often called the "Hurst Phenomenon," is identified by the fact that R/S scales as s^H where $H > 0.5$.

Feder (1988) has shown that the local fractal dimension, d_{FL}, of the trace of an FBM, which is a self-affine curve, is related to H by $d_{FL} = 2 - H$, $0 < H < 1$. In other words, H obtained from the R/S analysis gives rise to the fractal dimension of the time series under investigation.

Experimental

The experimental facilities are outlined. The procedures are described for operating these facilities and for carrying out the measurements and computations.

Facilities

Figure 3 depicts the experimental facilities. The fluidized bed consisted of a columnar section and a distributor; the column was fabricated from "Plexiglass" to permit visual observation. The bed had a diameter of 0.0508 m and a height of 0.6096 m. The distributor comprised a wire net (opening of 42 mesh or 0.354×10^{-3} m) and an alumina bead packed bed. Sand particles were fluidized by water and air. The physical properties of water, air and sand, and the experimental conditions are summarized in Table 1.

Pressure taps were installed on the wall of the bed column at three different heights. The outside opening of each pressure tap was connected to one of the two input channels of a differential pressure transducer (Enterprise Model CJ3D), which produced

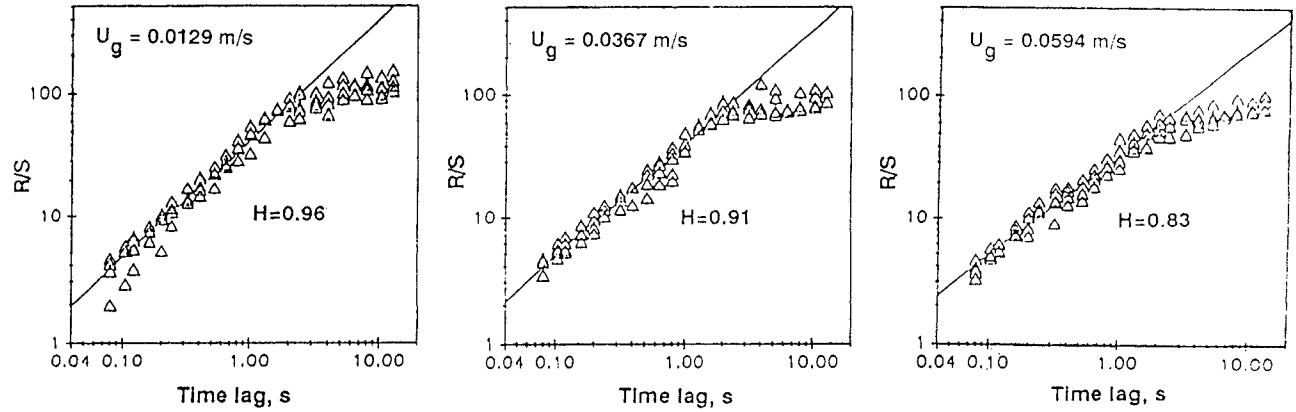

Figure 6. Typical Pox diagrams for pressure fluctuation signals at various superficial gas velocities.
$U_\ell = 0.056$ m/s; probe no. 2 (0.1302 m)

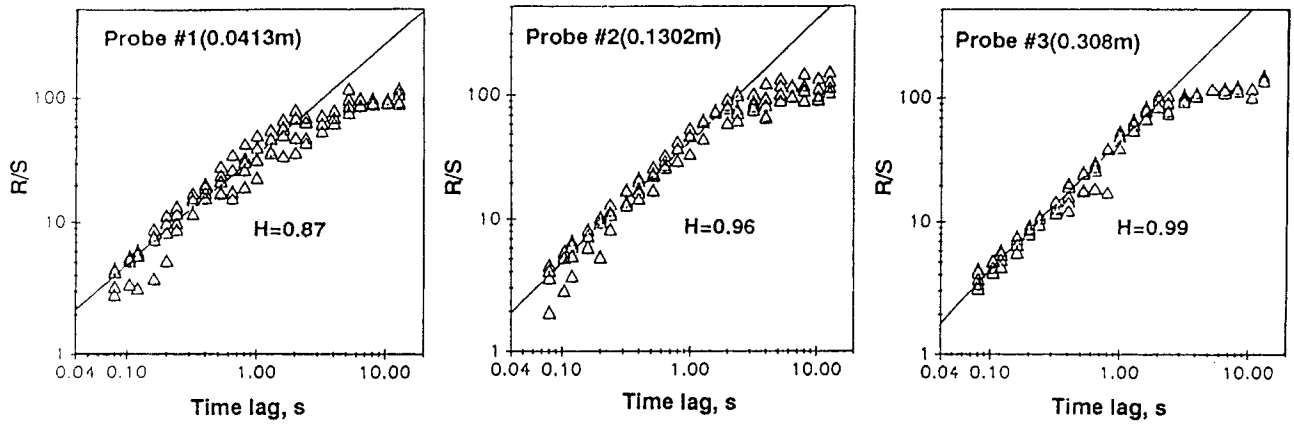

Figure 7. Typical Pox diagrams for pressure fluctuation signals at different probe heights.
$U_\ell = 0.056$ m/s; $U_g = 0.0129$ m/s

an output voltage proportional to the pressure difference between two channels. The remaining channel was exposed to the atmosphere. The working capacity of the transducer was ±34.5 kPa (±5 psi). Signals were processed with the aid of a Nicolet digital oscilloscope, a Zenith personal computer, and a mainframe computer (IBM 3084).

Procedures

The pressure fluctuations in the bed were detected by connecting the pressure tap to the pressure transducer. The voltage-time signal, corresponding to the pressure-time signal, from the transducer was fed to the recorder at the selected sampling rate of 0.008 s. A typical sample consisted of 1984 points. This combination of sampling rate and sample length ensured capturing of the full spectrum of hydrodynamic signals from the gas-liquid-solid fluidized bed, typically 25 Hz. The signals were processed off-line.

Results and Discussion

Typical signals recorded from the pressure transducer are traced in Figure 4 with the superficial velocity of the fluidizing gas as the parameter and in Figure 5 with the probe location as the parameter. Note that each tracing of the recorded signals at a given superficial velocity contains wavelike signals with various frequencies and random signals. In other words, each tracing is composed of a wavelike or sine component and a random or stochastic component. The variance or the magnitude of each signal increases with the increase in the superficial velocity. The trend for the amplitude to increase with the air flow rate was expected; it was visually observed that the bubble size became appreciably larger when the air flow rate was increased.

Figures 6 through 8 show the log-log plots of R/S against time lag; these plots are known as the "Pox diagrams" (Mandelbrot and Wallis, 1969a). For each time lag, the R/S has been computed by using five different starting times; this is evident from the presence of five data points, some of which are overlapping at each lag. These plots demonstrate that the Hurst exponent, H, tends to decrease (the local fractal dimension, d_{FL}, tends to increase) with the increase in the gas velocity for a given probe location and a constant liquid velocity. This could be attributed to the fact that at a low gas velocity, the viscous effect renders the bubble movements less irregular, thereby leading to a high level of persistency in the pressure fluctuation signals. It is highly plausible that the contrary can be expected at a high gas velocity, thereby leading to a decrease in the level of persistency, thus decreasing H. The effect of the increase in the liquid velocity, U_ℓ, with the other operating conditions fixed is not very

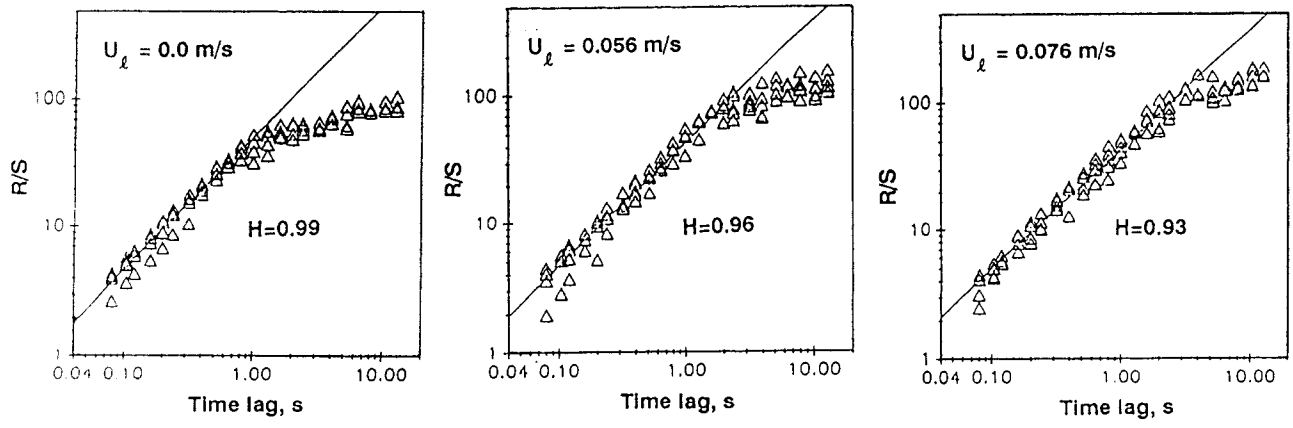

Figure 8. Typical Pox diagrams for pressure fluctuation signals at various superficial liquid velocities.
$U_g = 0.0129$ m/s; probe no. 2 (0.1302 m)

Table 2. Hurst Exponent under Various Operating Conditions*

Gas velocity m · s^{-1}	Probe No.	Hurst Exponent, H Liquid Velocity, m · s^{-1} 0	0.056	0.076
0.0129	1	0.99	0.87	0.92
	2	0.99	0.96	0.93
	3	0.98	0.99	0.90
0.0366	1	0.90	0.86	0.87
	2	0.84	0.91	0.84
	3	0.94	0.99	0.92
0.0594	1	0.88	0.76	0.80
	2	0.90	0.83	0.82
	3	0.99	0.99	0.85

*Fractal dimension, $d_{FL} = 2\text{-H}$

apparent with the present setup for signal detection. Nevertheless, Table 2 does indicate that a slight tendency exists for H to decrease and equivalently d_{FL} to increase with the increase in U_g. This could be due to the decrease in the residence time of gas bubbles, thus causing the movement of the bubbles to be less persistent. At any given set of gas and liquid velocities, H tends to increase (d_{FL} tends to decrease) with the probe height. This is attributable to the growth of bubble sizes through coalescence and expansion as the bubbles move up in the bed; consequently, the bubble movements are more persistent near the top than near the bottom of the bed.

The power spectral density functions (PSDF's) have also been computed for the pressure fluctuation signals. Figure 9 illustrates two typical examples of the experimentally obtained psdf's. The obvious, yet most important, feature of the power spectral densities obtained in all runs is the presence of one or more sharp peaks; see Figure 9a or 9b. This is indicative of the presence of one or more periodic components in the pressure fluctuation signals as mentioned earlier.

Another feature observable in the Pox diagrams (Figures 6 through 8) is the presence of a break in every R/S curve. Through simulated examples, Mandelbrot and Wallis (1969b) have attributed such a break to the presence of a periodic component. Furthermore, they have pointed out that the break occurring in the R/S curve at the time lag corresponds to the dominant frequency of the periodic component; in other words, a time series consisting of both random and periodic components will produce an R/S curve with a break. This paper has also revealed that the time lag at which the R/S curve breaks corresponds to the peak frequency, especially in the low frequency range, of the respective spectral density function. Mandelbrot and Wallis (1969b) have also stated that for high-frequency peaks, the R/S curve occasionally can fail to yield an apparent break; instead, the data points, corresponding to various starting times for R/S computation, become very compact or close to each other. For example, the spectral density in Figure 9b has two major peaks, one at a relatively low frequency of approximately 1 Hz and the other at a relatively high frequency of approximately 5 Hz. Its R/S curve has a break at the lag corresponding to the low-frequency peak and exhibits compactness of data points at the lag corresponding to the high-frequency peak. Thus, it is evident that R/S analysis not only confirms the presence of a random component following FBM but also predicts the presence of one or more periodic components.

To confirm the reproducibility of the Hurst exponents, H, ten experimental runs were conducted under identical operating conditions. The resultant values of H are listed in Table 3 along with their mean and standard deviation; evidently, H is statisti-

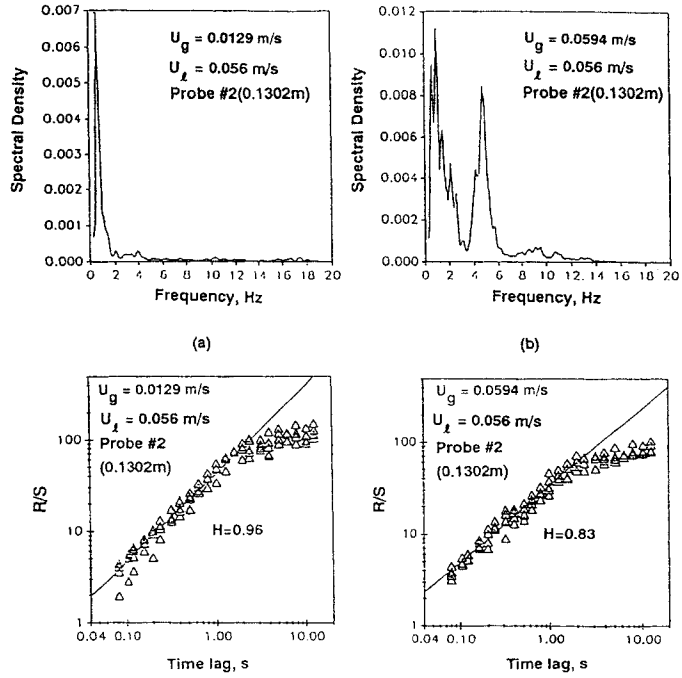

Figure 9. Comparison of the spectral densities with the corresponding Pox diagrams.

Table 3. Hurst Exponent for Different Experiments under Identical Operating Conditions*

Exp. No.	Hurst Exponent H
1	0.946
2	0.955
3	0.873
4	0.945
5	0.872
6	0.990
7	0.967
8	0.880
9	0.928
10	0.890
Statistics: Mean of $H = 0.925$, Standard Deviation of $H = 0.0428$	

*$U_\ell = 0.076$ m/s; $U_g = 0.0129$ m/s; probe no. 2 (0.1302 m)

cally reproducible. Since H appears to be a unique function of the operating conditions or fluidization regime, it may be regarded as a significant index for characterizing the quality of fluidization.

Concluding Remarks

A novel approach, based on the concept of temporal fractals, more specifically, fractional Brownian motion, has been adopted to analyze random pressure fluctuations from a three-phase fluidized bed. Unlike the classical Brownian motion and first-order Markov processes, FBM is capable of modeling long-term persistence or memory observable in such pressure fluctuations. These pressure fluctuations have been found to exhibit a Hurst phenomenon, characterized by the Hurst exponent, H, spanning between 0.7 and 1; these values correspond to the local fractal dimensions, d_{FL}, of 1.3 and 1.0, respectively. The results appear to indicate that FBM is a highly versatile and pragmatic model for analyzing time series evolving from complex flow systems like a three-phase fluidized bed and that it encompasses the classical Brownian motion and is capable of representing long-term correlation often present in such time-series data.

Acknowledgment

This is contribution #90-323-J, Department of Chemical Engineering, Kansas Agricultural Experiment Station, Kansas State University, Manhattan, KS.

Notation

$B(t)$ = classical Brownian motion
$B_H(t)$ = fractional Brownian motion
$c(t, u)$ = cumulative departure of the time series from its mean
D = diffusivity for classical diffusion
D_H = anomalous diffusivity for fractal diffusion
d_{FL} = local fractal dimension
$R(t, s)$ = sequential range
S = sequential standard deviation
s = time lag
t = time
U_g = superficial gas velocity
U_ℓ = superficial liquid velocity
u = time lag
$X(t)$ = time series

Literature Cited

Bailie, R. C., L. T. Fan, and J. J. Stewart, "Uniformity and Stability of Fluidized Beds," *Ind. Eng. Chem.*, **53**, 567 (1961).
Epstein, N., "Hydrodynamics of Three-phase Fluidization," *Handbook of Fluids in Motion*, N. P. Cheremisinoff and R. Gupta, eds., Ann Arbor Science, Ann Arbor, MI, 1165 (1983).
———, "Three-Phase Fluidization: Some Knowledge Gaps," *Can. J. Chem. Eng.*, **59**, 649 (1981).
Fan, L. T., T. C. Ho, S. Hiraoka, and W. P. Walawender, "Pressure Fluctuations in a Fluidized Bed," *AIChE J.*, **27**, 388 (1981).
Fan, L. T., and H. P. Newcomer, "Oxygen Transfer in Three Phase Fluidized Beds," *Adv. in Biotech.*, I. M. Moo-Young, ed., p. 643, Pergamon Press, New York (1981).
Feder, J., *Fractal*, p. 149, Plenum, New York (1988).
Hurst, E. H., "Methods of Using Long-term Storage in Reservoirs: I," *Proc. Instn. of Civil Engrs.*, **5**, 519 (1956).
Kang, W. K., J. P. Sutherland, and G. L. Osberg, "Pressure Fluctuations in a Fluidized Bed With and Without Screen Cylindrical Packings," *Ind. Eng. Chem. Fundam.*, **6**, 499 (1967).
Lirag, R. C., and H. Littman, "Statistical Study of the Pressure Fluctuations in a Fluidized Bed," *AIChE Symp. Ser.*, **67**, 116 (1971).
Mandelbrot, B. B., and J. W. van Ness, "Fractional Brownian Motions, Fractional Noises and Applications," *SIAM Rev.*, **10**, 422 (1968).
Mandelbrot, B. B., and J. R. Wallis, "Some Long-run Properties of Geophysical Records," *Water Resources Res.*, **5**, 321 (1969a).
Mandelbrot, B. B., and J. R. Wallis, "Robustness of a Rescaled Range R/S in the Measurement of Noncyclic Long Run Statistical Dependence," *Water Resources Res.*, **5**, 967 (1969b).
Moritomi, H., S. Mori, K. Araki, and A. Moriyama, "Periodic Pressure Fluctuations in a Gaseous Fluidized Bed," *Kagaku Kogaku Ronbunshu*, **6**, 392 (1980).
Muroyama, K., and L. S. Fan, "Fundamentals of Gas-Liquid-Solid Fluidization," *AIChE J.*, **31**, 1 (1985).
Neogi, D., L. T. Fan, N. Yutani, R. Nassar, and W. P. Walawender, "Effect of Superficial Velocity on Pressure Fluctuations in a Gas-Solid Fluidized Bed: A Stochastic Analysis," *Appl. Stochastic Models and Data Analysis*, **4**, 13 (1988).
Ostergaard, K., "Three-Phase Fluidization," *Fluidization*, J. F. Davidson and D. Harrison, eds., Chap. 18, p. 751, Academic Press, New York (1971).
Pietgen, H. O., and D. Saupe, eds., *The Science of Fractal Images*, p. 21, Springer-Verlag, New York (1988).
Shah, Y. T., *Reaction Engineering in Direct Coal Liquefaction*, Chap. 5, p. 213, Addison-Wesley, Reading, MA (1981).
Shuster, W., and P. Kisliak, "The Measurement of Fluidization Quality," *Chem. Eng. Prog.*, **48**, 455 (1952).
Sutherland, K. S., "The Effect of Particle Size on the Properties of Gas-fluidized Beds," *AEC Res. and Devel. Report*, ANL-6907, Argonne National Lab., Argonne, IL (1964).
Swinehart, F. M., "A Statistical Study of Local Wall Pressure Fluctuations in Gas Fluidized Column," PhD Diss., Univ. of Michigan, Ann Arbor (1966).
Whitehead, A. B., D. C. Dent, and C. H. McAdam, "Fluidization Studies in Large Gas-solid Systems. Part V: Long and Short Term Pressure Instabilities," *Powder Technol.*, **18**, 231 (1977).
Winter, O., "Density and Pressure Fluctuations in Gas Fluidized Beds," *AIChE J.*, **14**, 427 (1968).
Yutani, N., L. T. Fan, and J. R. Too, "Behavior of Particles in a Liquid-solids Fluidized Bed," *AIChE J.*, **29**, 101 (1983).

Manuscript received Jan. 26, 1990, and revision received July 31, 1990.